Hindawi
Advances in Civil Engineering
Volume 2023, Article ID 9856915, 1 page
https://doi.org/10.1155/2023/9856915

Retraction

Retracted: Simulation of Migration Law of Organic Pollutants in Circulating Wells

Advances in Civil Engineering

Received 3 October 2023; Accepted 3 October 2023; Published 4 October 2023

This article has been retracted by Hindawi following an investigation undertaken by the publisher [1]. This investigation has uncovered evidence of one or more of the following indicators of systematic manipulation of the publication process:

(1) Discrepancies in scope
(2) Discrepancies in the description of the research reported
(3) Discrepancies between the availability of data and the research described
(4) Inappropriate citations
(5) Incoherent, meaningless and/or irrelevant content included in the article
(6) Peer-review manipulation

The presence of these indicators undermines our confidence in the integrity of the article's content and we cannot, therefore, vouch for its reliability. Please note that this notice is intended solely to alert readers that the content of this article is unreliable. We have not investigated whether authors were aware of or involved in the systematic manipulation of the publication process.

Wiley and Hindawi regrets that the usual quality checks did not identify these issues before publication and have since put additional measures in place to safeguard research integrity.

We wish to credit our own Research Integrity and Research Publishing teams and anonymous and named external researchers and research integrity experts for contributing to this investigation.

The corresponding author, as the representative of all authors, has been given the opportunity to register their agreement or disagreement to this retraction. We have kept a record of any response received.

References

[1] X. Li, J. Zhang, and Z. Yang, "Simulation of Migration Law of Organic Pollutants in Circulating Wells," *Advances in Civil Engineering*, vol. 2022, Article ID 7342604, 12 pages, 2022.

Hindawi
Advances in Civil Engineering
Volume 2022, Article ID 7342604, 12 pages
https://doi.org/10.1155/2022/7342604

Research Article

Simulation of Migration Law of Organic Pollutants in Circulating Wells

Xiaojie Li, Jianwei Zhang, and Zhuojing Yang

Center for Hydrogeology and Environmental Geology, China Geological Survey, Baoding 071051, Hebei, China

Correspondence should be addressed to Jianwei Zhang; chegs_jianwei@st.btbu.edu.cn

Received 6 May 2022; Revised 21 June 2022; Accepted 30 June 2022; Published 20 July 2022

Academic Editor: Ramadhansyah Putra Jaya

Groundwater resources are one of the most important freshwater resources for human beings. The protection of groundwater resources is an important measure for human survival. Therefore, it is extremely important to discuss the treatment of pollutants in groundwater. The purpose of this paper is to simulate and analyze the migration law of organic pollutants using the experimental circulating well. In the analysis, this paper uses the gas-liquid-solid three-state model to simulate the pollutants for organic pollutants. It independently analyzes pollutants in different states. For the movement law, this paper not only simulates the vertical transition circulation well in the laboratory but also simulates the transport law of pollutants in the well. The experimental results show that in the laboratory environment, the simulated value of the circulation well designed in this paper is not far from the actual value, and the accuracy rate is more than 90%. And according to the movement law of organic pollutants, it is found that the variable flow rate and the dispersion, porosity, and thickness of the skin have a great influence on the migration of pollutants.

1. Introduction

Groundwater is one of the most valuable natural resources supporting human health, economic development, and ecosystem diversification. In dry and semiarid areas with relatively few surface water sources, groundwater plays an irreplaceable role as an important source of water resources. However, in the process of industrialization and urbanization, with the depletion of groundwater and the deterioration of water quality, especially serious groundwater pollution, various pollutants attached to the surface infiltrate into groundwater from circulating wells. Pollutants in the groundwater seep in. The problem of organic pollution directly endangers the survival and safety of human beings.

In recent years, the organic pollution of groundwater has become a hot spot in groundwater scientific research, attracting the attention of scholars. The only way for contaminants to intrude into groundwater is through circulation wells, so organic contaminants in circulation wells are becoming more and more noticeable. Volatile organic pollutants are different from inorganic pollutants. They have high toxicity, fire resistance, and volatility. Their movement, metamorphism, and form are affected by their properties and the surrounding geological environment, and repair work is extremely difficult. The innovation of this paper is to simulate the mechanical energy of the organic pollutants' migration law in the circulating well and find out the organic pollutants' migration law. It plays an important role in the scientific simulation and prediction of groundwater pollution, effective governance and improvement of groundwater pollution status, and the maintenance of sustainable economic and social development and protection of the ecological environment.

2. Related Work

With the rapid development of economy, the increasing intensity of industrial and agricultural production and human activities, the problem of soil and groundwater pollution has become increasingly prominent. Organic

contamination of soil and groundwater is of great concern to researchers and governments. Liu et al. G found that the radical-based advanced oxidation process (AOP) has received increasing attention in water and wastewater treatment, and its radicals face the challenges of high operating costs and potential secondary pollution [1]. Liang et al. found that the detection of organic contaminants in water media is essential to ensure the quality and safety of water resources. Here, they described a sticky nanomat made of crystallizable fluorescent polymers for easy detection of toxic contaminants in water. Adhesive nanomats can rapidly detect organic contaminants within seconds [2]. Novikov analyzed long-term observational data (2003–2018) from 625 stations to determine the relationship between organochlorine pesticides and pollutants in the entire ocean and six selected regions. He used mathematical statistics and GIS analysis methods to process the data and presented the concentration distribution map of the inspected pollutants [3]. Shi et al. found that antibiotics have become the dominant organic pollutants in water resources, and efficient removal of antibiotics is the primary task of protecting the water environment. They synthesized various photocatalysts using a combination of hydrothermal synthesis and partial annealing. The results show that the removal rate is about 80% [4]. Lakshmi et al. found that the global population is increasing, and the world may experience severe freshwater shortages. Water treatment and recycling methods are the only options for obtaining fresh water for decades to come. Therefore, there is an urgent need to develop a suitable, inexpensive, and rapid wastewater treatment technology and reuse or conservation method in this century [5]. Scholars have discovered the shortage of water resources and the threat of organic pollutants to water resources, but they have not given specific and effective methods on how to remove organic matter.

For the study of groundwater resources, most scholars focus on the study of circulating wells. Zeng et al. found that groundwater has been increasingly used in open-loop soil-coupled heat pump systems as an alternative to realizing environmentally friendly geothermal systems for space heating and/or cooling [6]. Kurtul and Duran studied the application of circulating wells in water resource restoration [7]. Sulikowska et al. aimed to describe the temporal and spatial characteristics of extreme warm days (WDs) and warm periods (WSs) in summer and extremely cold days (CDs) and cold periods (CSs) in winter in Alaska from 1951 to 2015. They also determined the role of atmospheric circulation in its occurrence [8]. Morozov considered groundwater flow near vertical circulation wells. He presented a solution to the problem of steady-state and transient groundwater flow near vertical circulation wells in anisotropic aquifers, taking into account both skin and wellbore storage effects at pumping and injection intervals [9]. However, it can be found that many scholars have a wide range of research, focusing on the regulation of the overall environment of water resources, and there is still a lack of research on the establishment of pollutant transport models.

3. Calculation Based on the Migration Law of Organic Pollutants in Circulating Wells

3.1. Status and Harm of Organic Pollutants

3.1.1. Status of Organic Pollutants. With the continuous development of China's economy and society and the continuous improvement of urbanization level, the impact of human activities on groundwater resources has become more and more serious [10]. Compared with the "water quantity type" water shortage, the "water quality type" water shortage due to the pollution of groundwater or the poor quality of natural water resources is gradually becoming an important factor of water shortage. Organic chemical products will leak in the processes of refining, use, and storage, coupled with the random discharge of human beings, which makes the problem of organic pollution in soil and groundwater continue to aggravate. The main sources of groundwater organic pollution include the use of pesticides and fertilizers, oil spills, and seepage, and the random placement and discharge of organic wastes by factories and enterprises. Organic pollutants refer to pollutants composed of natural organic substances in the form of carbohydrates, proteins, amino acids, and fats and some other biodegradable synthetic organic substances [11]. Developed countries have attached great importance to the problem of organic pollution of groundwater and invested a lot of money in investigation and research. It has successively carried out investigations on organic pollution of drinking water, and developing countries are still in their infancy [12]. Water pollution caused by organic pollutants is shown in Figure 1.

As shown in Figure 1, after the end of the 20th century, scholars mainly investigated the polluted areas in the region. After the investigation of residual organic pollutants in the region, they gradually carried out risk assessment, remediation, research on treatment technology, and the transfer and conversion mechanism of organic pollutants. Through the sampling analysis of the Geological Survey, the results show that VOC can be detected almost in the water-bearing layer [13].

At present, the research on the migration and transformation mechanism of VOCs in China mainly focuses on the adsorption process and the degradation process, and the research on groundwater volatile organic pollutants is also gradually carried out. The research on organic pollution of groundwater is still in its infancy, and the research on the migration, transformation, and restoration mechanism of organic pollutants is still immature. It mainly studies its migration and transformation law in the geological environment, decontamination prevention and control technology, etc., and its application range is not large [14].

In recent years, due to the increasing influence of human activities and the rapid development of industry and agriculture, the role of petroleum organic pollutants on groundwater pollution has become more and more obvious. A large number of organic chemical products are directly or indirectly derived from the petrochemical industry. On the

Figure 1: Water pollution from organic pollutants.

one hand, petrochemical products provide convenience for human life, and on the other hand, they also bring many pollution problems. In the processes of oil refining, transportation, and use, phenomena such as foaming and liquid leakage will occur, and various organic pollutants with high toxicity will invade the environment and cause extremely serious pollution to soil and groundwater [15].

3.1.2. Harm of Organic Pollutants. Most of the organic pollution are more toxic or potentially toxic to the ecological environment and human health. Polluted soil and groundwater often contain a variety of pollutants, but their physical and chemical properties are different [16]. Organic pollutants can change the chemical composition of water bodies, increase the biological oxygen demand (BOD) and chemical oxygen demand (COD) of water bodies, and change the pH of water bodies [17]. The organic pollutants in the water body are further decomposed by anaerobic organisms and produce hydrogen sulfide, ammonia, mercaptan, and other products with pungent odor [18]. Since organic pollutants contain a variety of highly toxic substances, they are potentially harmful to humans [19]. The harm of organic pollutants to the human body is shown in Figure 2.

As shown in Figure 2, organic pollutants paralyze the human central nervous system, which may lead to cancer in some organs, weaken the function of the nervous system, and reduce their own immunity. Although the toxicity of perchloroethylene is less than that of trichloroethylene, its harm to humans cannot be ignored [20].

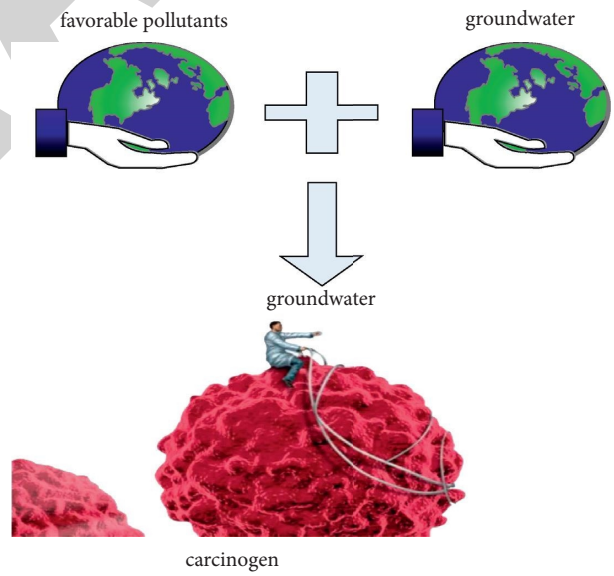

Figure 2: Harm of organic pollutants to human body.

3.2. Substance Exchange between Three Phases of Gas-Liquid-Solid. VOCs migrate in soil through leaching, volatilization, and diffusion and escape into water and atmosphere. It may be absorbed by the ecosystem and migrate out of the geological body, causing great harm to the air, surface water, groundwater, ecosystem, and human life. Therefore, it is extremely important to study the migration and transformation mechanism of volatile organic pollutants in circulating wells [21, 22].

The distribution of volatile organic pollutants in the gas-water-solid three phases includes the distribution of

pollutants between the water phase and the gas phase, the distribution between the water phase and the solid particles, and the accumulation at the interface between the water phase and the gas phase. In the unsaturated state, there is an equilibrium between the three phases of gas, liquid, and solid, mainly the water-gas two-phase distribution equilibrium combined with the water-solid two-phase distribution equilibrium [23]. Henry's law is one of the basic laws of physical chemistry. It can be expressed as follows: at a certain temperature and equilibrium state, the solubility of a gas in a liquid (expressed in mole fraction) is proportional to the equilibrium partial pressure of the gas. Henry's law can be used to express the material exchange balance between the water-gas phase as shown in the following formula:

$$C_a = HC_w. \tag{1}$$

In the formula, C_a is the pollutant concentration in the gas, C_w is the pollutant concentration in the water, and H is the Henry coefficient.

For the exchange of pollutants between the water phase and the solid phase, a linear formula is often used as follows:

$$q_s = K_d C_W, \tag{2}$$

where q_s is the concentration of pollutants on the surface of solid particles.

Soil particles are often of different sizes, different surface areas, and different organic matter contents. Linear formulas cannot realistically describe the material distribution between the water-solid phase. Freundlich equation is a chemical engineering term published in 1995. Therefore, the nonlinear adsorption isotherm formula, Freundlich formula, is used to describe the following formula:

$$q_s = K_F C_W^{1/n}. \tag{3}$$

In the formula, K_F is the distribution coefficient, and the diffusion of pollutants in the gas phase is not considered. Assuming that the gas phase is static, the pollutants migrate with water in the circulating well, which can be expressed by the following formula:

$$R_t \frac{\partial C_W}{\partial_t} = -v_a \frac{\partial C_W}{\partial_a} + D_W \frac{\partial^2 C_W}{\partial_a^2}. \tag{4}$$

In the formula, R_t is the hysteresis coefficient.

The retardation coefficient is the ratio of the velocity of groundwater seepage to the velocity of pollutant migration, and it is an important parameter to calculate and evaluate the migration behavior of pollutants in groundwater. The distribution and material exchange between the water-gas-solid three phases determine the migration of VOCs in the circulating well. When the interphase material exchange is in equilibrium, the retardation coefficient is used to represent the retardation of material exchange, as shown in the following formula:

$$R_t = 1 + \frac{\rho k_d}{\theta_w} + \frac{\theta_a H}{\theta_w}. \tag{5}$$

In the case of different water content and different pollutant transport mediums, the expression of the retardation coefficient is different, and the migration of volatile organic pollutants with the gas phase in the circulating well is as shown in the following formula:

$$R_t = 1 + \frac{\rho k_d}{\theta_w} + \frac{\theta_a H}{\theta_w}. \tag{6}$$

Recent studies have shown that, due to the accumulation of pollutants on the water-air interface, the experimentally measured coefficient values are larger than the predicted values obtained from formula (4). The retardation coefficient represents the retardation caused by the material exchange between water-gas and water-solid particles during the transport of pollutants. After comprehensive consideration, the delay coefficient of pollutants moving with gas is shown in the following formula:

$$R_t = 1 + \frac{\rho k_d}{\theta_a H} + \frac{\theta_W}{\theta_a H} + \frac{K_i A_i}{\theta_a}. \tag{7}$$

K_i is the adsorption coefficient (cm) of VOCs accumulated at the water-air interface, and A_i is the effective water-air interface area.

3.3. Water Infiltration Characteristics. Water infiltration is an important way for pollutants to penetrate the circulation well and enter the aquifer. Understanding the characteristics of water infiltration under the condition of sufficient water supply is extremely important for the study of solute transport in the unsaturated zone [24]. Infiltration is divided into two processes: non-water infiltration and water infiltration: the initial water supply intensity of infiltration is less than the infiltration capacity without water, which is the non-water infiltration stage. With the increase of infiltration amount, when the water supply intensity is equal to the infiltration capacity, it reaches the time of infiltration water accumulation, and the surface begins to accumulate water and enters the accumulation water infiltration stage under pressure conditions.

Some scholars have introduced unsaturated soil-water flow as shown in the following formula:

$$q = -K(\theta \nabla \psi), \tag{8}$$

where ψ is the soil-water potential and ∇ is the nabla operator.

3.3.1. Continuity Formula for Soil Water Movement (Conservation of Mass). Assuming that the soil water is incompressible, and the soil is isotropic, the initial conditions for the studied problem are as follows:

$$\begin{cases} \theta(z,0) = \theta_i(z) \\ h(z,0) = h_i(z). \end{cases} \tag{9}$$

In the case of evaporation intensity as a function of topsoil θ or h, the three types of boundary conditions are as follows:

$$D(\theta)\frac{\partial\theta}{\partial z} - K(\theta) = a\theta + b. \quad (10)$$

The basic formula for water transport in the one-dimensional unsaturated zone is as follows:

$$\frac{\partial\theta}{\partial t} = \frac{\partial}{\partial z}\left[D(\theta)\frac{\partial\theta}{\partial z}\right]. \quad (11)$$

In order to facilitate the application of the above basic formulas, in practical applications, appropriate formula forms are selected according to specific conditions to simplify complex problems.

3.4. Migration Model of Organic Pollutants in Water Circulation Wells. Groundwater Circulation Well (GCW) was called "well aeration and well treatment technology" in the early days. After that, some scholars added a treatment device to the well and developed a special filter for delaying clogging. Groundwater circulating well technology can also be combined with other technologies, such as bioremediation, surfactant technology, and oxidation technology. After it is repaired by GCW technology, the removal rate of trichloroethylene in the polluted groundwater is 90%. By the late 1990s, GCW technology was basically mature and had made great progress. The GCW technology is shown in Figure 3.

As shown in Figure 3, circulating well technology treats volatile organic pollutants in groundwater through groundwater circulation. It is connected with the inner well through the fixing device, and the inner and outer wells are sealed. The method utilizes an aeration pump to aerate the inner well, the gas forms a mixture with the groundwater in the inner well, and the density decreases and migrates upward. When it reaches the upper flower tube of the outer well, it flows back to the aquifer, and the gas carrying pollutants is discharged from the upper tail gas outlet through the gas-water separator. At the lower flower tube, there is a density difference inside and outside the well, and the groundwater outside the well continuously enters the well. Through continuous aeration, dissolved pollutants enter the inner well and are removed by aeration blow-off. The process of oxygen species transfer is shown in Figure 4.

As shown in Figure 4, the vertical circulation of groundwater may promote the disorder of the medium with water layer and promote the desorption of pollutants, and the transfer of oxygen species between the two phases of gas-water will increase the dissolved oxygen content in the groundwater. It has the potential to enhance biodegradation in situ. When the permeability of the aquifer is good, more water can be recharged into the aquifer, and the restoration effect is significantly improved.

The influence area around a single GCW is predicted by establishing a numerical model, and its governing formula is as follows:

$$\frac{\partial}{\partial r}\left(2\pi rK\frac{\partial h}{\partial r}\right) + \frac{\partial}{\partial z}\left(2\pi rK\frac{\partial h}{\partial z}\right) = 0. \quad (12)$$

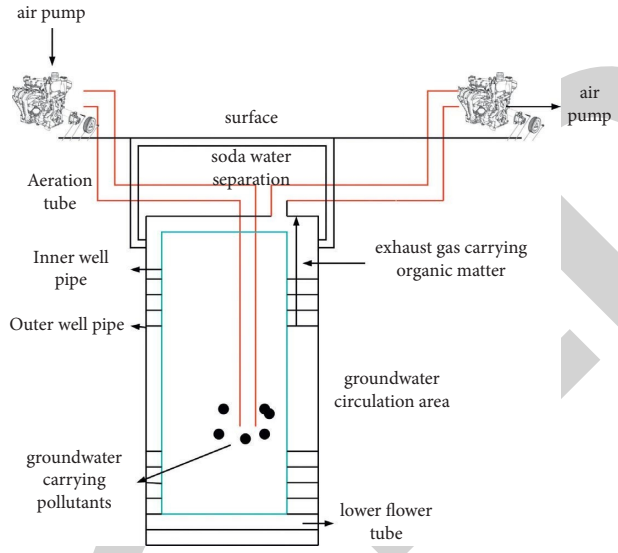

Figure 3: GCW technology.

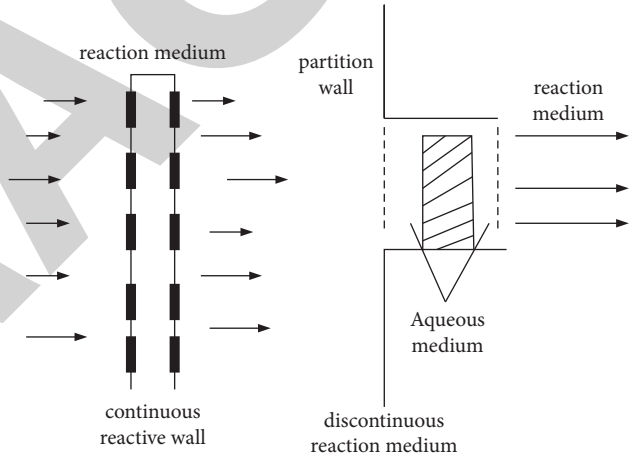

Figure 4: The process of oxygen species transfer.

r represents the influence radius in the horizontal direction; h represents the head of the piezometer; ∂h and ∂z represent the radial and vertical permeability coefficients.

The simulation conditions of the two-dimensional model of the groundwater circulation well are uniform and isotropic steady flow, the thickness of the aquifer and the Darcy velocity are constants, and the basic theoretical formula is the Laplace formula. The capture band width is as follows:

$$\mathrm{CZW} = \frac{Q}{UB}\left(\frac{N}{2} - I_r\right). \quad (13)$$

In the formula, Q is the total flow; B is the thickness of the aquifer; U is the Darcy velocity; N is the number of circulating wells; IT is the total exchange flow of the system. The processing efficiency is as follows:

$$\eta = \frac{\eta_{SP}}{1 - I_{avg}(1 - \eta_{SP})}. \quad (14)$$

In the formula, η_{SP} represents the single-channel pollutant removal rate; I_{avg} represents the average flow exchange.

The three-dimensional model simulation conditions of the circulating well are uniform, anisotropic, and steady flow with zero horizontal groundwater velocity. The theoretical formula is Lagrange's law and Darcy's law. Darcy's law clarifies the equation of steady-state flow energy loss in porous media such as soil, which is the basic law for studying the movement of saturated soil moisture. The flow at any point s is as follows:

$$s(a,b,z) = -J[a\cos(\theta) + b\sin(\theta)]. \tag{15}$$

In the formula, J represents the hydraulic gradient; θ represents the number of the well pipe; b represents the thickness of the aquifer.

The applicability of groundwater circulation well technology is as follows: in contrast to actual on-site treatment technologies (enhanced biomedical technology, etc.), no toxic or partially refractory intermediate compounds are introduced into the aquifer. Under the influence of the water cycle, dissolved oxygen is intensified. The content of groundwater increases, and the decomposition of aerobic microorganisms in that case is enhanced. It does not generate lateral water pressure or cause the spread of pollutants, and the organic removal efficiency of high pollutant concentrations can reach up to 98%.

3.5. Migration Law Based on Multiphase Flow Calculation Principle. Organic pollutants are mainly molecules composed of two elements C and H combined with other elements (N, 0, S). An important feature of organic pollutants is the functional group with basic physical and chemical properties reflected in its molecular structure. Different types of organic pollutants have different functional groups, which determine the basic physicochemical properties of these substances.

Organic pollutants can enter the soil in various ways and infiltrate into the aquifer under the action of gravity and capillary force. After entering the aquifer, organic pollutants usually exist in the form of nonaqueous phase liquids (NAPLs) because of their low solubility, liquids that do not mix with the water in the circulation well and below the water surface. Such liquids are often referred to as nonaqueous liquids. The transformation of NAPLs is shown in Figure 5.

As shown in Figure 5, the existence forms of NAPLs in underground aquifers mainly include free state, dissolved state, gaseous state, and residual state. There is mutual conversion between the four forms, and the residual saturation is closely related to the properties of the medium. It is often the most difficult part of the subsurface medium to repair and remove.

There are many forms of organic pollutants after entering groundwater, among which NAPL phase is the main form of existence in groundwater. Organic pollutants also undergo corresponding transformations between different

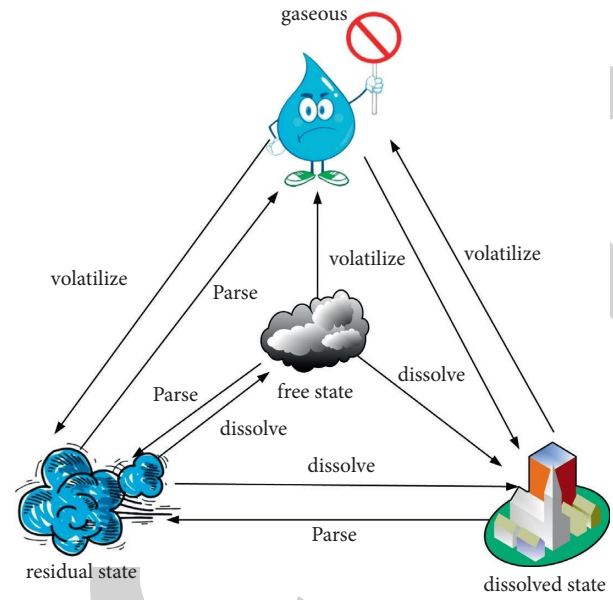

Figure 5: Transformation of NAPLs.

phases. It includes evapotranspiration, dissolution, and adsorption, so that dynamic equilibrium reactions occur among the four states of gaseous state, free state, dissolved state, and residual state. These processes contain many complex influencing factors. Among them, the physical and chemical properties of NAPLs, the heterogeneity of the medium, and the hydraulic conditions of the fluid are all important factors that affect the migration and transformation of NAPLs between phases.

The multiphase flow system in TMVOC software includes three parts: water phase, NAPL phase, and incompressible gas. The software can simulate any combination of single phase, two phases, or three phases among the three components. Due to the differences in the saturation and thermodynamic conditions of the three parts, the migration and distribution process will be accompanied by the mutual transformation between the phases. The expression of its mass and energy conservation formula in TMVOC software is as follows:

$$\frac{d}{d_t}\int_{v_n} M^K dV_n = \int_{r_n} F^K \bullet n d\tau_n + \int_{r_n} q^K dV_n. \tag{16}$$

Among them, V_n represents the unit volume, and τ_n is the area through which the fluid passes.

The total mass of the water and gas phases in a unit volume can be expressed as follows:

$$M^K = \varphi \sum_{\beta} S_\beta \rho_\beta A_\beta^K. \tag{17}$$

Among them, φ is the porosity of the porous medium, and S_β is the saturation of the β phase. The total mass of the NAPL phase per unit volume can be expressed as follows:

$$M^K = \varphi \sum_{\beta} S_\beta \rho_\beta A_\beta^K + M_{ads}^K. \tag{18}$$

Among them, S_β in the above formula is the saturation of the β phase, and M_{ads}^K is the instantaneous reverse adsorption of the K group by the soil medium.

For the numerical simulation of multiphase flow, relative permeability model and capillary pressure model are important factors to determine its migration and distribution in soil-groundwater system. In this paper, the three-phase flow permeability, Stone model, and capillary pressure Parker model are used.

The expression for the relative permeability model is as follows:

$$k_{rg} = \frac{S_g - S_{gr}}{1 - S_{wr}}. \tag{19}$$

Among them, S_g and S_{gr} are the relative permeability of water phase, gas phase, and NAPL phase, respectively. The expression for the capillary pressure model is as follows:

$$S_{wr} = \frac{S_w - S_m}{1 - S_m}. \tag{20}$$

Among them, S_m is the residual saturation of the liquid phase, and S_w is the capillary pressure between the NAPL phase and the gas phase.

The migration behavior of multiphase flow in the underground environment obeys Darcy's law and forms a multiphase flow system under the action of gravity and capillary pressure. In the process of multiphase flow, the components will transform into each other and diffuse in various forms. The diffusion behavior of multiphase flow refers to the distribution method under the condition of variable phase saturation, and the diffusion and transport are carried out in a fully coupled manner.

In this paper, by analyzing the time-space variation of pollutants, the adsorption-desorption mechanism of pollutants was found out. It is combined with the seepage column experiment to simulate the migration law of pollutants with different pollution pathways. In this paper, a groundwater solute migration model is established to predict the migration trend of pollutants. After entering the geological medium, volatile organic pollutants mainly include migration and transformation processes such as convective dispersion, adsorption-desorption, degradation, and volatilization. The main factors affecting its migration are VOCs own characteristics, hydrogeological conditions, geological engineering geological conditions, groundwater, etc.

4. Simulation of Hydrodynamic Field of Circulating Well

4.1. Hydrodynamic Field Model of Vertical Circulation Well. In the confined aquifer, a vertical well with a radius of r_w includes an upper and lower pumping section and a water injection section, and the two sections are sealed with plugs at the same time to form a closed cavity. The upper pumping section maintains the pumping volume of $-Q$ flow rate, the lower water injection section maintains the water injection volume of $+Q$ flow rate, and a pressure difference is formed in the cavity, thereby forming a circulation field from bottom to top. The mathematical model of vertical circulation well established in this paper is established based on the following assumptions:

(1) The vertical circulation well device is installed in the confined aquifer

(2) The aquifer is laterally unbounded

(3) The thin-wall effect of vertical circulation wells is not considered

(4) Under natural conditions, groundwater in the aquifer does not flow, that is, there is no background flow of groundwater

This paper uses the ModelMuse software developed by the United States Geological Survey (USGS) to simulate a groundwater numerical model. ModelMuse is a software for simulating groundwater flow based on GoPhast. The software includes MODFLOW-2005, MODPATH, ZONEBUDGET, and other parts, and ModelViewer is a bundled software for postprocessing of the software. It enables graphic output and analysis of postsimulation results. The operating object is a three-dimensional model, and the operability for meshing and boundary condition setting of the model is flexible. The formula can be used to specify the spatial data value of the global and individual objects. And the specified value has nothing to do with the spatial and temporal discretization of the model, and the user can redefine it. The setting for the aquifer can be restricted, unrestricted, or a combination of restricted and unrestricted, which can well satisfy the user's operation setting for the model.

In this paper, combined with the scale of the laboratory experiment and the characteristics of the selected research unit, a numerical model of the laboratory experiment of the indoor vertical circulation well is established. It takes the bottom as the 0 reference plane, the model length is 1.02 m, the width is 0.06 m, and the height is 0.9 m. The main boundary conditions involved in the model are the injection and pumping sections in the vertical circulation well. They are given flow boundaries, which are generalized by the Flow and Head Boundary package (FHB) module in ModelMuse. Both sides of the model are defined as fixed head boundaries. Using the Time-Variant Specified-Head package (CHD) module in ModelMuse to generalize, the initial head height of the model is defined as 94 cm. On the plane, the circulation well is arranged at the center, and the model is divided into 6 rows, 61 columns, and 18 layers. The grid size of the model gradually transitions from the outer periphery of the well axis, from cell1: $0.005\,\text{m} \times 0.005\,\text{m}$ to cell2: $0.03\,\text{m} \times 0.03\,\text{m}$, and then to cell3: $0.035\,\text{m} \times 0.035\,\text{m}$, and the subdivision is divided into three levels. The parameter settings of the reference model for laboratory experiments are shown in Table 1.

4.2. Model Numerical Verification. In order to determine the accuracy of the numerical model, it needs to be verified and compared with the analytical solution under the same parameters. It provides the numerical simulation results of the

Table 1: Value list of model parameters.

Parameter	Value	unit
Well radius r_w	0.05	m
Thickness of aquifer D	0.94	m
Radius of influence r'	0.5	m
Extract that distance d between the upper and lower bottom of the section and the surface of the aquifer d, d_e	0.19, 0.29	m
The distance l between the upper and lower bottoms of the injection section and the aquifer surface, l, l_e	0.64, 0.74	m
Distance between center points of extraction section and injection section ∇L	0.45	m
Q flow	0.1	m^3/h
Horizontal and vertical hydraulic conductivity K_r, K_z	3×10^{-3}	m/s
Anisotropy ratio K_r/K_z	1	

water head of the reference model at a depth of $z = 0.575$ m and 0.675 m at different horizontal distances. It is compared with the analytical solution of the head value calculated by the formula under the same conditions. Under the numerical model, some parameters are determined, and the accuracy of the model is analyzed by software. The results are shown in Figure 6.

Uncertainty analysis of the magnitude of the numerical simulation flow should be made, keeping all parameters of the numerical model the same as those of the experimental model. It only changes the flow rate and finally selects numerical simulation parameters that are close to the actual flow rate. A scatter plot of the simulated water head height and the experimental water head height is drawn, respectively, to observe the correlation between the two, as shown in Figure 7.

4.3. Hydrodynamic Field Results. In the establishment of the numerical model under the indoor scale, the flow parameter is set as the actual flow rate, and the water head monitoring points are set up in the model, and the number of the monitoring points is larger than the number of the water head monitoring points in the experimental model tank. It also includes the location of the experimental water head monitoring point, which is calculated by numerical simulation. It obtains the water head height in each monitoring point, and the monitoring results are shown in Figure 8. The variation law of the water head at different depths is the same, and the fitting effect of the head reduction at $z = 0.8$ and $z = 0.7$ is better. As the depth from the aquifer surface increases, the experimental water head height value is lower than the numerical simulation water head height value.

The vertical circulation well device forms an elliptical groundwater circulation field with the pumping section as the central axis during operation. In order to quantitatively calculate the groundwater circulation velocity of the circulation wells in the area, this paper takes the position of the straight line where the center points of the monitoring holes A4~F4 of the model tank are located as the x-axis. The position of the straight line where the central axis of the vertical circulation well is located is the y-axis, which establishes a Cartesian coordinate system. The water head monitoring holes of the entire model tank are divided into four areas according to the location of the pumping section, and at the same time, in each area, three points are selected to mark the monitoring points of the known water level. It calculates the average groundwater flow velocity in each area of the hydrodynamic field separately. The head heights of the selected monitoring points in the divided areas are shown in Table 2.

The groundwater flow velocity at the center point of each triangle is obtained, as shown in Table 3.

From Table 3, it can be concluded that the average groundwater flow rates in areas 1, 3, 2, and 4 are approximately the same. It is left-right symmetrical with the position of the central axis of the drawing section as the symmetrical axis. $V_y > V_x$ in areas 1 and 3, $V_x > V_y$ in areas 2 and 4, and the average velocity of groundwater in areas 1 and 3 is greater than that in areas 2 and 4, a difference of about 3 times. This paper analyzes the causes of $V_y > V_x$ in areas 1 and 3, and the vertical circulation well device forms reverse flow during operation. It circulates back from the bottom injection section to the position where the upper extraction section is located, and there is a partial head loss.

5. Simulation of Migration Law of Organic Pollutants in Circulating Wells

According to the derivation and calculation of the above model, this section mainly discusses the influence of variable flow rate and the dispersion, porosity, and thickness of the skin region on the contamination of the tandem layer based on the semianalytical model. For the following research analyses, the default model parameters are shown in Table 4.

5.1. Influence of Variable Flow on Pollutant Transport. In this section, $k1 = 1$ and $k2 = 1$ are set in the semianalytical model calculation, which means that the influence of variable flow on the transport of pollutants under the action of the skin is not considered. Figure 9(a) shows the penetration curves of pollutants at $r = 2$ m when λ takes different values, and the MO solution (steady flow) is also included in the figure for comparative analysis. It can be seen from the figure that the larger the attenuation index λ of the flow, the smaller the concentration of the pollutant breakthrough curve. It shows that the larger the decay index is, the slower the pollutants move. This is mainly due to the fact that the larger the flow decay index, the faster the flow decay, resulting in a faster decrease in the radial groundwater velocity. In addition, by comparing the breakthrough curve of variable flow rate with the solution of steady flow of MO, it can be found that the concentration of breakthrough curve under the condition of variable flow rate is lower than that of steady flow. It shows

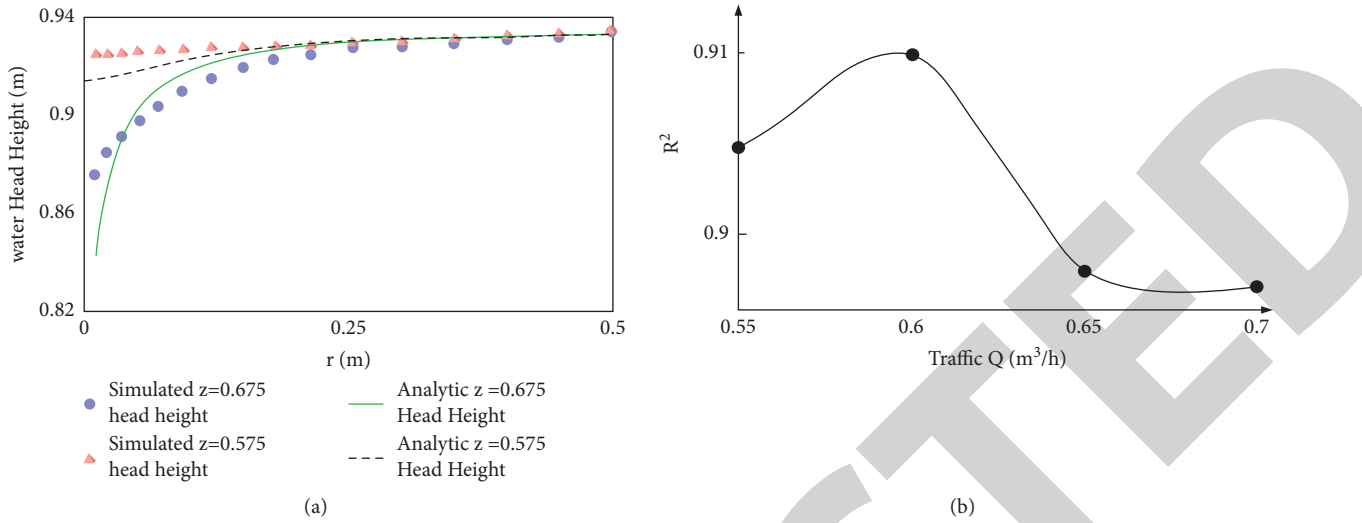

Figure 6: Numerical verification analysis of the model. (a) Comparison of the simulated and analytical solutions of the water head values at different depths of the reference model. (b) Flow rate Q vs. R graph.

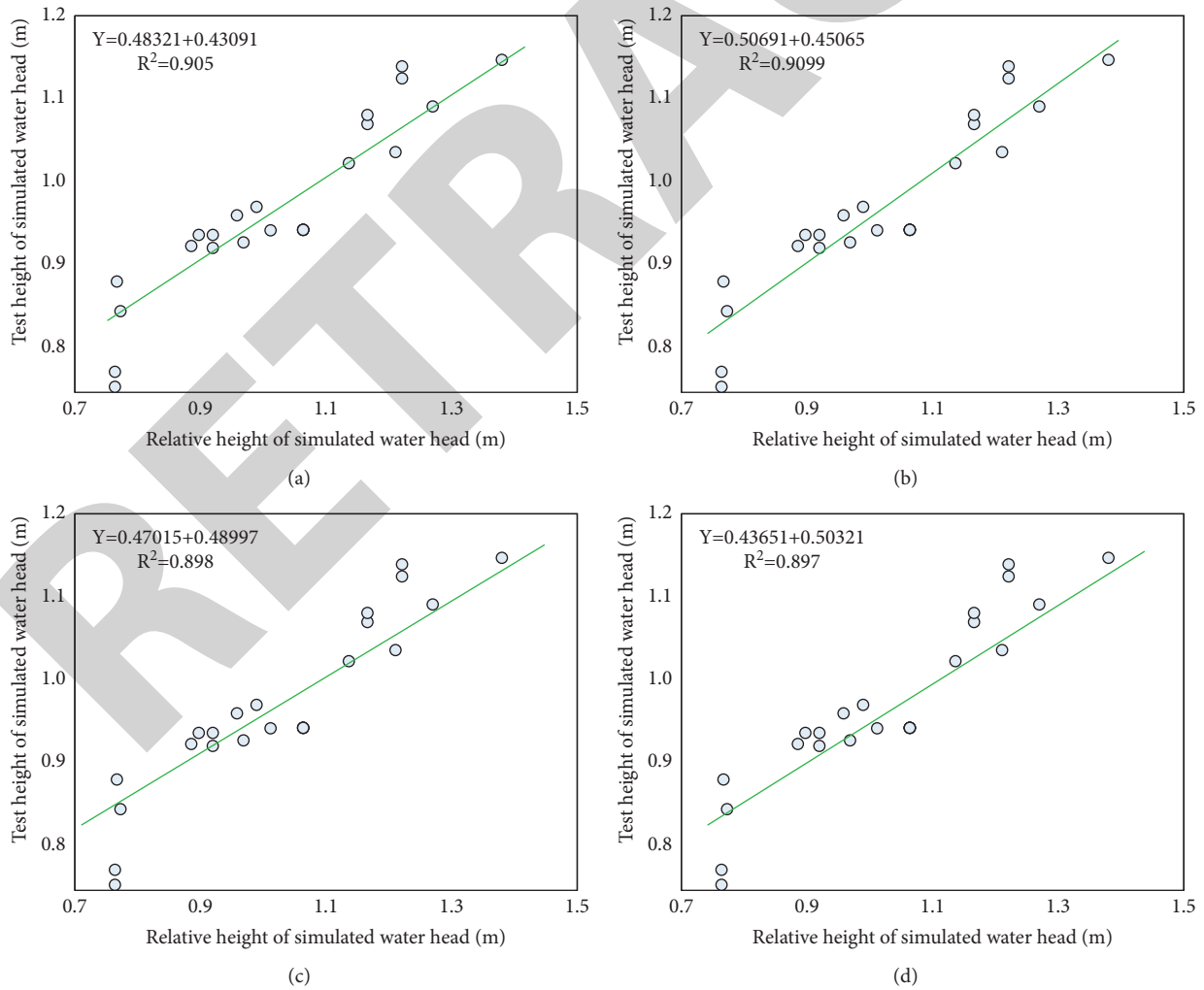

Figure 7: Scatter plot of R^2 analysis with different flow sizes. (a) $Q = 0.55\ m^3/h$. (b) $Q = 0.6\ m^3/h$. (c) $Q = 0.65\ m^3/h$. (d) $Q = 0.7\ m^3/h$.

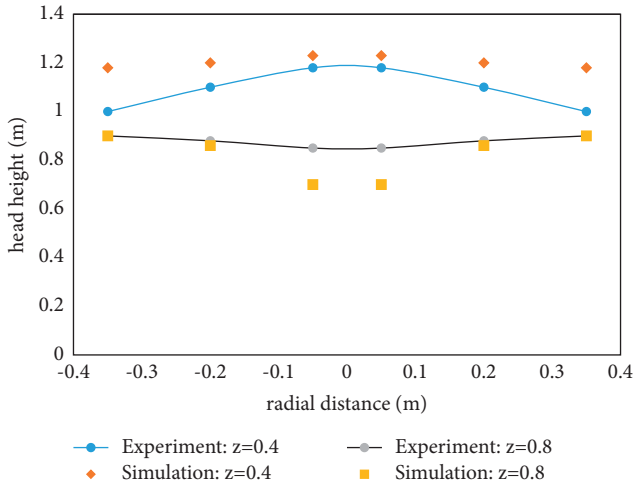

Figure 8: Fitting diagram of experimental head value and numerical simulation head value.

Table 2: Head height values of water head monitoring points in different areas.

Zone	Water head height monitoring point	Height of water head (cm)
1	H1	84.33
	H2	76.9
	H3	96.5
2	H4	113.97
	H5	115.17
	H6	102.7
3	H7	84.63
	H8	74.67
	H9	95.77
4	H10	112.73
	H11	115.17
	H12	102.27

Table 3: Water velocity at the center point.

Central point	V_x (m/h)	V_y (m/h)	V (m/h)
1	1.78	2.54	3.10
2	1.14	0.18	1.15
3	2.13	3.02	3.69
4	1.06	0.37	1.12

that variable flow has a greater impact on the radial transport of pollutants; especially for cascade pollution, the attenuation of flow will lead to a smaller range of pollutant transport. This has played a positive role in protecting groundwater resources.

Figure 9(b) shows the penetration curves of pollutants at $r = 2$ m when $Q2$ takes different values. It can be seen from the figure that the smaller the final stable flow rate $Q2$ is, the smaller the concentration of the breakthrough curve of pollutants is, indicating that the smaller the $Q2$ is, the slower the pollutants migrate. This is mainly because the smaller the final steady flow, the greater the attenuation of the radial groundwater velocity, so the speed of pollutant transport is

Table 4: Parameter values in the model.

Parameter	Value
Aquifer thickness (m)	10
Well radius (m)	0.1
Epidermal area radius (m)	1
The porosity of the movable zone of the aquifer	0.3
Porosity in the movable zone of the epidermis	0.3
Radial dispersion of aquifer (m)	0.5
Radial dispersion of epidermis (m)	0.5

smaller. For example, the permeability of the epidermal region near the well tube is reduced due to microbial clogging. The final steady flow rate of the tandem is also reduced, especially when the dissolved oxygen content is higher, the less permeable the skin area near the well tubing, the smaller the final tandem flow rate. Therefore, reducing the final interlayer flow is also of positive significance for the protection of groundwater resources.

Among them, A is the influence of different flow attenuation exponents on the penetration curve under the condition of variable flow; B is the influence of the final steady flow on the penetration curve.

5.2. Influence of Skin Dispersity and Porosity on Radial Pollutant Transport. This section analyzes the influence of skin effect on radial pollutant transport under variable flow rate conditions. Figure 10(a) shows the penetration curves of pollutants at $r = 2$ m when $k1$ takes different values. The dimensionless parameters $k1$ are 0.2, 1, and 5, respectively, and $k2 = 1$. Here, if $k1 < 1$ means $\alpha1 < \alpha2$, and the smaller the $k1$ is, the smaller the dispersion of the epidermis is. If $k1 = 1$ and $k2 = 1$, it represents the case of no epidermis. Other parameters in the model are $Q1 = 30\ m^3/d$, $Q2 = 15\ m^3/d$, $\lambda = 0.5/d$. Comparing the penetration curves in the three cases, the value of the solution of this model is smaller than that of the MO solution in the middle and late stages, which is mainly caused by the decrease of the flow rate. At the same time, it is also found that, with the increase of the dispersion of the epidermal region, the concentration of the penetration curve also increases. It shows that the dispersity in the epidermis area has a great influence on the radial pollutant migration, and if the dispersity is greater than that of the aquifer, it will promote the contamination of the tandem layer. However, it has an inhibitory effect on the case where the dispersion is less than that of the aquifer.

Figure 10(b)shows the pollutant penetration curves (BTCs) at $r = 2$m when $k2$ takes different values. In addition, the figure also considers the other two cases as a comparison, which is the solution of MO steady flow without skin. The dimensionless parameters $k2$ are 3/5, 1, and 3, respectively, and $k1 = 1$. Here, if $k2 < k1$ means $\theta1 > \theta2$, the smaller the $k2$, the greater the porosity of the epidermis. Other parameters in the model are $Q1 = 30/d$, $Q2 = 15/d$, $\lambda = 0.5/d$. It can be seen from Figure 10 that the value of the solution of this model in the middle and late stages is smaller than that of the MO solution, which is mainly caused by the decrease in flow. It shows that the

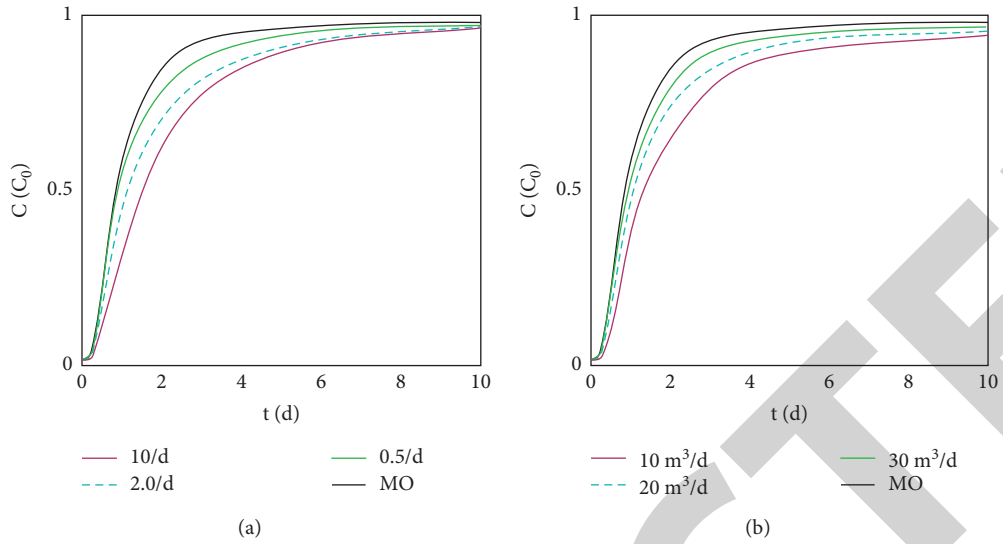

Figure 9: Effect of variable flow rate on pollutant transport.

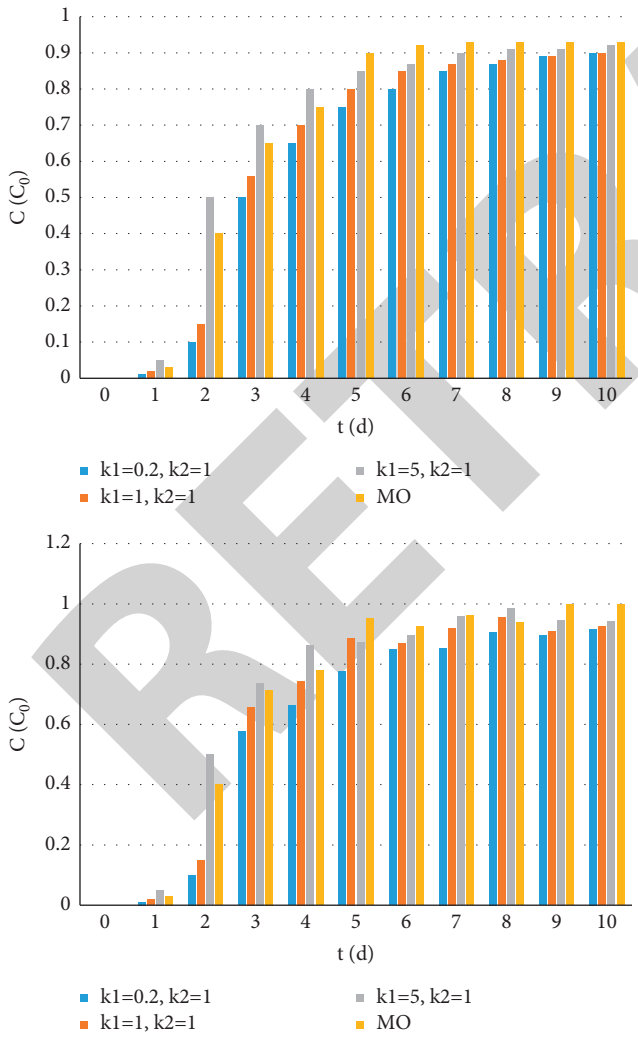

Figure 10: Effects of skin dispersity and porosity on radial pollutant transport. (a) A Effect of different dispersions on penetration curves under variable flow conditions. (b) The effect of different porosity on the penetration curve of radial pollutants under the condition of variable flow.

decrease of flow rate has a great influence on radial pollutant transport. In addition, as $k2$ increases, the value of the penetration curve also increases gradually. This indicates that changes in the porosity of the skin region can affect the penetration curve of pollutants. This is because the larger the $k2$ is, the smaller the porosity of the skin area is, and the larger the groundwater flow rate is. This in turn results in faster contaminant transport and causes and increases breakthrough curve concentration values.

5.3. Influence of Skin Thickness on Radial Pollutant Transport. The previous two sections have analyzed the variation of the contaminant concentration distribution curve and the penetration curve caused by the variable flow rate as well as the dispersion and porosity of the skin region. This section mainly analyzes the influence of the thickness of the skin on the transport of pollutants under the condition of variable flow. Contaminant breakthrough curves (BTCs) at a distance of $r = 2$ m from the water injection well when r1 takes different values. Dimensionless parameters $k1 = 0.2$, 1, 5, $k2 = 3/5$, 1, 3, other parameters are $r1 = 0.5$ m, 1 m, $Q1 = 30/$ d, $Q2 = 15$/d, $\lambda = 0.5$/d. When $k1 = 5$ and $k2 = 3$, as $r1$ increases, the concentration of pollutants in the penetration curve increases. However, when $k1 = 0.2$ and $k2 = 3/5$, as $r1$ increases, the concentration of solute becomes smaller. The experimental results show that different thicknesses also have a certain influence on the transport of pollutants.

6. Conclusion

In this paper, a theoretical model of radial cascading pollution considering the skin effect is established under the condition of variable flow rate. The semianalytical solution of the model is obtained by Laplace transform and Stehfest numerical reversal method. This paper can effectively control the repair scope and repair effect of the vertical circulation well by studying the influencing factors of the hydrodynamic field of the vertical circulation well, which provides a basic reference

for the operation in the actual site. As mentioned above, groundwater is one of the important components of the water circulation system, and its research significance is self-evident. This paper takes groundwater pollution and vertical circulation wells as important research contents. For the hydrodynamic field of vertical circulation wells, the theoretical analysis established by mathematical physical formulas and the comparison and verification of numerical simulation results are the main research methods to solve the dynamic field of vertical circulation wells in groundwater.

Data Availability

No data were used to support this study.

Conflicts of Interest

The authors declare that there are no conflicts of interest regarding the publication of this article.

Acknowledgments

This work was supported by Isolation well forming technology and influence radius amplification method of multifilter circulating well system (National Key R&D Projects 2020YFC1808302).

References

[1] G. Liu, S. You, Y. Tan, and N. Ren, "In situ photochemical activation of sulfate for enhanced degradation of organic pollutants in water," *Environmental Science & Technology*, vol. 51, no. 4, pp. 2339–2346, 2017.

[2] G. Liang, F. Ren, H. Gao, F. Zhu, B. Z Wu, and Q. Tang, "Sticky nanopads made of crystallizable fluorescent polymers for rapid and sensitive detection of organic pollutants in water," *Journal of Materials Chemistry*, vol. 5, no. 5, pp. 2115–2122, 2017.

[3] M. A. Novikov, "Persistent organic pollutants in barents sea bottom sediments," *Water Resources*, vol. 48, no. 3, pp. 439–448, 2021.

[4] H. Shi, T. Zheng, Y. Zuo, Q. Wu, and P Zhang, Y. Fan and Y. Tontiwachwuthikul, Synthesis of Cu3P/SnO2 composites for degradation of tetracycline hydrochloride in wastewater," *RSC Advances*, vol. 11, no. 53, pp. 33471–33480, 2021.

[5] S. S. Lakshmi, S. Rajesh, and R. P. Kumar, "Removal of organic pollutants from textile dye wastewater by advanced oxidation process," *International Journal of Civil Engineering & Technology*, vol. 9, no. 4, pp. 452–461, 2018.

[6] Y. Zeng, W. Zhou, and J. LaMoreaux, "Single-well circulation systems for geothermal energy transfer," *Environmental Earth Sciences*, vol. 76, no. 7, p. 296, 2017.

[7] A. Kurtul and M. Duran, "The correlation between lymphocyte/monocyte ratio and coronary collateral circulation in stable coronary artery disease patients," *Biomarkers in Medicine*, vol. 11, no. 1, pp. 43–52, 2017.

[8] A. Sulikowska, J. P. Walawender, and E. Walawender, "Temperature extremes in Alaska: temporal variability and circulation background," *Theoretical and Applied Climatology*, vol. 136, no. 3-4, pp. 955–970, 2019.

[9] P. E. Morozov, "Groundwater flow near a vertical circulation well with a skin-effect," *Water Resources*, vol. 48, no. 5, pp. 737–745, 2021.

[10] D. M. Kahler and Z. J. Kabala, "Rapidly pulsed pumping accelerates remediation in A vertical circulation well model," *Water*, vol. 10, no. 10, p. 1423, 2018.

[11] M. Zhang, C. Yang, Z. Zhang et al., "Tungsten oxide polymorphs and their multifunctional applications," *Advances in Colloid and Interface Science*, vol. 300, Article ID 102596, 2022.

[12] K. Tu, Q. Wu, and H. Sun, "A mathematical model and thermal performance analysis of single-well circulation (SWC) coupled ground source heat pump (GSHP) systems," *Applied Thermal Engineering*, vol. 147, no. 54, pp. 473–481, 2019.

[13] Q. Wu, Kl Tu, H. Sun, and C Chen, "Investigation on the sustainability and efficiency of single-well circulation (SWC) groundwater heat pump systems," *Renewable Energy*, vol. 130, no. JAN, pp. 656–666, 2019.

[14] S. Wei, L. Yuanzhou, Z. Ke, and Z. Tuanfeng, "Numerical simulation of forced external circulation standing column well based on CFD," *Procedia Engineering*, vol. 205, no. 41, pp. 3178–3185, 2017.

[15] N. Liu and Q. Gao, "Temperature prediction of oil well during circulation of compressible aerated fluids with leakage," *Modelling, Measurement & Control, B*, vol. 87, no. 2, pp. 92–96, 2018.

[16] P. Shan and X. Lai, "Influence of CT scanning parameters on rock and soil images," *Journal of Visual Communication and Image Representation*, vol. 58, no. 1, pp. 642–650, 2019.

[17] A. Sadeghi, H. Hassanzadeh, and T. G. Harding, "A comparative study of oil sands preheating using electromagnetic waves, electrical heaters and steam circulation," *International Journal of Heat and Mass Transfer*, vol. 111, no. aug, pp. 908–916, 2017.

[18] E. A. E. A. A. E. a S. Elhishi, A. Abo-Elfetoh, and S. Elhishi, "Pollution reduction using intelligent warning messages in VANET," *Journal of Intelligent Systems and Internet of Things*, vol. 3, no. 2, pp. 57–67, 2021.

[19] F. Rigét, A. Bignert, B. Braune et al., "Temporal trends of persistent organic pollutants in Arctic marine and freshwater biota," *Science of the Total Environment*, vol. 649, no. 1-1662, pp. 99–110, 2019.

[20] O. S. Reshetnyak, V. N. Reshetnyak, K. G. Vlasov, and K. G. Myagkova, "Long-term dynamics of the river water quality in the northern dvina basin (northwestern Russia)," *Water Resources*, vol. 45, no. S2, pp. 93–98, 2018.

[21] M. Nowakowska and K. Szczubiałka, "Photoactive polymeric and hybrid systems for photocatalytic degradation of water pollutants," *Polymer Degradation and Stability*, vol. 145, no. nov, pp. 120–141, 2017.

[22] V. A. Zubarev and R. M. Kogan, "Ecological conditions of watercourses in the middle amur lowland in the areas of drainage reclamation," *Water Resources*, vol. 44, no. 7, pp. 940–951, 2017.

[23] F. X. Kong, Z. P. Wang, Z. Ji et al., "Organic fouling of membrane distillation for shale gas fracturing flowback water desalination: a special interest in the feed properties by pretreatment," *Environmental Science Water Research & Technology*, vol. 5, no. 7, pp. 1339–1348, 2019.

[24] A. F. Troyanskaya and A. V. Velyamidova, "Persistent organic pollutants in subarctic lakes in the extreme North of European Russia," *Water Resources*, vol. 44, no. 4, pp. 635–644, 2017.